Ultrasonics Sonochemistry 74 (2021) 105568

Contents lists available at ScienceDirect

Ultrasonics Sonochemistry

journal homepage: www.elsevier.com/locate/ultson

Complexation of maltodextrin-based inulin and green tea polyphenols via different ultrasonic pretreatment

Shuyi Li [a,b], Dan Lei [a], Zhenzhou Zhu [a,b,*], Jie Cai [a,b], Maela Manzoli [c], Laszlo Jicsinszky [c], Giorgio Grillo [c], Giancarlo Cravotto [c,*]

[a] National R&D Center for Se-rich Agricultural Products Processing Technology, School of Modern Industry for Selenium Science and Engineering, Wuhan Polytechnic University, Wuhan 430023, China
[b] Key Laboratory for Deep Processing of Major Grain and Oil, Ministry of Education, Wuhan 430023, China
[c] Department of Drug Science and Technology, University of Turin, Turin 10125, Italy

ARTICLE INFO

Keywords:
Inulin
Tea polyphenols
Complexation
Ultrasonic treatment
Identification

ABSTRACT

Ultrasound has been applied in food processing for various purpose, showing potential to advance the physical and chemical modification of natural compounds. In order to explore the effect of ultrasonic pretreatment on the complexation of inulin and tea polyphenols (TPP), different frequencies (25, 40, 80 kHz) and output power (40, 80, 120 W) were carried out. According to the comparison in particle size distribution and phenolic content of different inulin-TPP complexes, it was indicated that high-intensity ultrasonic (HIU) treatment (25 kHz, 40 W, 10 min) could accelerate the interaction of polysaccharides and polyphenols. Moreover, a series of spectral analysis including UV–Vis, FT-IR and NMR jointly evidenced the formation of hydrogen bond between saccharides and phenols. However, the primary structure of inulin and the polysaccharide skeleton were not altered by the combination. Referring to field emission scanning electron microscopy (FESEM), the morphology of ultrasound treated-complex presented a slight agglomeration in the form of bent sheets, compared to non-treated sample. The inulin-TPP complex also revealed better stability based on thermogravimetric analysis (TGA). Thus, it can be speculated from the identifications that proper ultrasonic treatment is promising to promote the complexation of some food components during processing.

1. Introduction

Ultrasound (US), a mechanical/acoustic wave, can be converted from electrical energy to mechanical energy, inducing physical and/or chemical changes of different dimensions [1,2]. Ultrasound is usually characterized in terms of wavelength, frequency and intensity. According to the frequency, it has been classified into three categories: power ultrasound (20–100 kHz), high-frequency ultrasound (100 kHz-1 MHz), and diagnostic ultrasound (1–500 MHz) [3]. In food processing, ultrasound less than 100 kHz is often used with high power intensity from 1 to 1000 W/cm^2. The high-intensity/low-frequency ultrasound, which produces cavitation effect, can advance the physical and chemical modifications of compounds [4,5]. Furthermore, compared to conventional processing technologies, ultrasound is often considered as a kind of emerging or non-thermal technique, which preserves the bioavailability of food components and improves their functional properties with high efficiency in food industry and agricultural production [6–10].

Nowadays, high-intensity ultrasonic (HIU) treatment has been widely applied to improve the functional properties of food proteins, including crop, bean and egg yolk protein isolates [11–13]. Moreover, it is indicated that ultrasonic pretreatment can intensify the hydrolysis or degradation of starch or some polysaccharides, further modifying their properties, such as gelation and rheological properties [14,15]. It is also found recently that ultrasound under special conditions is effective to accelerate the interaction of food components, inducing alteration on physicochemical and functional properties of foods. For example, Albano et al. (2020) demonstrated that ultrasound homogenization promotes the complexation of soy protein isolate and methoxyl pectin based on electrostatic interaction, which is potent to be emulsion stabilizers [16]. Greater interactions between protein and polysaccharide were observed in whey protein concentrate-pectin complexes with

* Corresponding authors at: School of Modern Industry for Selenium Science and Engineering, Wuhan Polytechnic University, No. 68 Xuefu South Road, Changqing Garden, 430023 Wuhan, China (Z. Zhu). Department of Drug Science and Technology, University of Turin, Via P. Giuria 9, 10125 Turin, Italy (G. Cravotto).
E-mail addresses: zhenzhouzhu@126.com (Z. Zhu), giancarlo.cravotto@unito.it (G. Cravotto).

https://doi.org/10.1016/j.ultsonch.2021.105568
Received 5 February 2021; Received in revised form 7 April 2021; Accepted 13 April 2021
Available online 18 April 2021

ultrasonic treatment, indicating reduced suspension viscosity and smaller size [17]. Intriguingly, it was further reported that lotus seed starch-green tea polyphenol complex with slow digestibility could be formed after treated by synergistic ultrasound and microwave [12]. Hence, utilization of ultrasound has been recognized as an effective strategy to improve food quality, which is considerably easy to industrialize and scale-up.

Since the concern on human health is growing and no cure or vaccine has been developed for COVID-19 disease yet, the demand of functional foods sharply increases in the market and the behavior of consumers will change to adapt to the innovations of food supply chain [18–20]. More and more food ingredients and active compounds supporting body's immune system have been consumed, such as vitamins and folate, polysaccharides and dietary fiber, lipids, peptides, and natural polyphenols [21]. Phenol-rich extracts obtained from plant resources or food processing by-products are generally accepted for its excellent performance in antioxidation, which have been widely used in food industry or cosmetics [22,23]. To be mentioned, the enrichment of food-derived polyphenols also depends on ultrasound-assisted extraction or other non-thermal technologies, which has promising application foreground [24]. Inulin, known as functional fructo-oligosaccharides or polysaccharides, mainly comes from natural resources, such as coneflower, chicory root and Jerusalem artichoke root [25]. The commonly present inulin contains two types: Fn type through fructosyl-fructose links, and GFn type with a glucose unit at the end of fructan chain [26]. It has been widely used for production of healthier food products or ingredients, being as sugar substitute, fat replacer or texture modifier [27]. However, inulins with high degree of polymerization (DP) lead to lower solubility and enhanced viscosity of food matrix, which restrict its application in food industry to some extent. Recently, we found that the complexation of inulin and polyphenol (e.g epicatechin and its oligomers) will strengthen the antioxidant activity and solubility of polysaccharides, broadening its usable range in foods. However, the absorption rate of polyphenols on inulin is limited, accompanied with low yield of the complex. Therefore, a food-acceptable strategy needs to be employed, improving the reaction efficiency of inulin and other small molecules.

In this study, ultrasound was introduced to advance the interaction of inulin and tea polyphenols in vitro systems with different frequencies and output power. In order to select the optimal ultrasonic condition and illustrate its positive effect on the complexation, the morphological and spectroscopic properties of the complex were identified by a series of characteristic methods.

2. Materials and methods

2.1. Chemicals and materials

Inulin extract was kindly offered by MB Med S.R.L (Torino, Italy), obtained from roots of *Taraxacum officinale* (L.), using maltodextrin as carrier. The green tea polyphenols were extracted from *Camellia sinensis* Kuntze (purity˃90%), which was mainly composed of epigallocatechin gallate (EGCG) and epicatechin gallate (ECG) referring to HPLC results and previous studies [28,29]. Folin-Ciocalteu reagent was purchased from Sigma Co. (USA). All other reagents used in this experiment are of analytical grade.

2.2. Ultrasonic treatments

In order to prepare inulin-polyphenol complex, 800 mg of inulin extract and 200 mg of tea polyphenols (TPP) were mixed and suspended in 15 mL of diluted water. The fully dissolved solution was exposed to different ultrasonic treatments and incubated for different time durations. Ultrasonic conditions involving 25 kHz (40 W, 80 W, 120 W), 40 kHz (40 W, 80 W, 120 W) and 80 kHz (40 W, 80 W, 120 W) were carried out, in which the optimal parameter was selected and applied to promote the formation of inulin-TPP complex. The untreated solution of inulin at the presence of TPP was set as control.

After incubation, the products were isolated through alcohol precipitation. Samples of complexes were further collected by centrifugation (4000 r/min, 10 min) and washed twice with 50% ethanol solution to remove the uncomplexed polyphenols. The final precipitates were freeze-dried and ground to powder, which was recorded in Fig. 2C.

2.3. Particle size analysis of ultrasound-treated mixtures

The ultrasound-treated and untreated solutions containing inulin, TPP and their complex were evaluated by 90Plus Particle size analyzer (Brookhaven Instrument Co., USA). The diameter distribution and average particle size of the product was obtained based on five parallel tests, which was collected at the wavelength of 675 nm.

2.4. Phenolic content determination

The total phenol content of inulin-TPP complex was measured by the Folin-Ciocalteu method referring to Li et al. (2020) with modifications, using gallic acid as standard [30]. 1 mL of Folin-Ciocalteu reagent was added into 0.5 mL of different samples (1 g/L), which was followed by addition of 1 mL of 7% Na_2CO_3 solution, and kept in dark for 90 min. The absorbance of the final solution was determined at wavelength of 760 nm, and the relative phenolic content of the complex could be calculated.

2.5. Ultraviolet–visible (UV–Vis) analysis

Based on the phenolic content of non-treated complex, the corresponding uncombined mixture of inulin and TPP can be prepared with same weight ratio. Then, three inulin-TPP complexes (1 g/L) from different ultrasonic treatments and their mixtures were determined on a UV–Vis spectrophotometer, recording from 200 to 800 nm (Cary 60 UV–Vis, Agilent Technologies, USA).

2.6. Fourier transform infrared (FT-IR) spectroscopy

The FT-IR spectra of four samples (three inulin-TPP complexes and one mixture) were measured by a spectrometer from 500 to 4000 cm^{-1} with scans 16 times and 8 resolutions respectively (NEXUS670, Nicolet, USA). 3 mg of samples was fully mixed with dried KBr (300 mg), and then pressed into tables for analysis.

2.7. Nuclear magnetic resonance (NMR) spectroscopy

The ultrasound-treated and untreated inulin-TPP complex were maintained over P_2O_5 in a vacuum for several days and deuterium exchange was performed thrice with 0.5 mL D_2O. ^1H NMR, ^{13}C NMR and correlation spectroscopy (COSY) spectra of samples were recorded in D_2O at 500 MHz (for ^1H NMR) or 125 MHz (for ^{13}C NMR) using a Jeol ECZR600 spectrometer, operating at 14 T and equipped with Jeol Royal Standard probe.

2.8. High performance gel permeation chromatography

The molecular weight distribution of different inulin-TPP complexes and their mixture, were observed by high performance gel permeation chromatography (GPC). Samples (0.2% w/w, dissolved by mobile phase) were examined by Agilent 1100 liquid chromatography, which was equipped with G1376A binary gradient pump, Agilent G137A injector, and G1328B differential refractive index detector. The type of column applied was PL aquagel-OH MIXED (7.5 mm × 300 mm, 8 μm). Conditions were as follows: flow rate at 0.9 mL/min, column temperature at 35 °C, and the mobile phase was 0.05 M of Na_2SO_4 [30].

2.9. Field emission scanning electron microscopy analysis

The morphological properties of different inulin-TPP complexes were characterized by field emission scanning electron microscopy (FESEM) analysis, using a Tescan S9000G FESEM 3010 microscope (30 kV) equipped with a high brightness Schottky emitter and fitted with Energy Dispersive X-ray Spectroscopy (EDS) by a Ultim Max Silicon Drift Detector (SDD, Oxford). For analysis, the powdered samples were deposited on a stub and inserted in the chamber by a fully motorized procedure. In order to avoid any modification, the samples of complex were not metallized and the secondary electron (SE) FESEM images have been acquired at 2 keV. It is worth noting that under these conditions the complexes were stable to prolonged exposition to the electron beam of the instrument.

2.10. Thermogravimetric analysis

The maximum decomposition rate and thermal stability of different inulin complexes was measured by thermogravimetric analysis (TGA), referring to the relationship between weight loss and heating time. The thermodynamic properties of four samples were obtained depending on Perkin Elmer TGA 4000 (New York, USA). Approximate 10.0 mg of samples were weighed in the tubes, heating from 30 °C to 800 °C at 10 °C/min, under 90 mL/min of argon atmosphere.

2.11. Statistical analysis

The data of particle size and phenolic content were expressed as mean ± standard deviations (SD). The statistical significance was defined as p less than 0.05, which was conducted using single factorial ANOVA with Origin 8.0 software.

3. Results and discussion

3.1. Effect of ultrasound on the complexation of inulin and TPP

Particle size distribution has been often used to define powder, granular material, or particles dispersed in fluid, associated with the relative amount, proportion and mass of compounds [31]. Thus, the complexation of inulin and TPP in solution was examined by dynamic light scattering in this study, indicating significant changes after ultrasonic treatment. It has been demonstrated that the formation of complex often leads to increased average diameter and wider molecular weight distribution compared to original substrates [32,33]. Moreover, ultrasound can facilitate the chemical combination of compounds, but depending on conditions [34,35]. Herein, there was a contrast effect of ultrasound with different frequencies on the complexation of inulin and TPP. According to Fig. 1, it was indicated that 25 kHz-ultrasound-treated solution possessed a significantly larger mean diameter (around 1084 nm at 40 W), and the particle size distribution of which was more condensed than the untreated inulin-TPP dispersed fluid. It was possibly caused by the cavitation effect of high-intensity ultrasound that transfers energy during the oscillation and rupture of bubbles, accelerating the aggregation and interaction of compounds. However, 40 and 80 kHz of ultrasound decreased the mean diameter of the solutes, further producing inulin-based solutions with more dispersive size distributions. This is owing to the ultrasonication with higher frequencies, which can generate more stable bubbles, presenting weaker cavitation effect and hindering the contact of substrates [36]. Another possibility could be that the intrinsic chain structure of inulin was destroyed by the specific ultrasound, decomposed to shorter saccharides. For example, ultrasound irradiation (20 kHz, 600 W) degraded the polysaccharide from blackcurrant fruit into smaller molecules, increasing the antioxidant activities but not changing the primary structure of polysaccharides [37]. The pectin can be also degraded and modified by ultrasound, presenting better properties and higher bioactivities [38].

In addition, the increase in the power of sonication caused the particles of inulin-TPP to shift toward smaller sizes, which was similar to the study of Chen et al. (2011) [39]. As the increase of vibration amplitude (40 ~ 120 W), the intensity of the bubble collapse was enhanced, resulting in the de-aggregation or de-gradation of the nanoparticles.

3.2. Optimal parameters of ultrasonic treatment for complexation

Based on the result of 3.1, it was implied that 10 min of ultrasound can be effective to facilitate the combination of inulin and TPP at 25 kHz (40 or 80 W). In order to identify the time-effect, 400 mg of inulin and 100 mg of TPP were dissolved in 10 mL of water, which was treated by ultrasound for different time periods. It was indicated that the mean diameter of particle size was increased at the beginning, which was followed by gradual decline in the second half of treatment (Fig. 2). The largest particles were obtained at 10 and 5 min for 40 and 80 W of ultrasound, respectively. Extending reaction time led to a slight de-aggregation of the complex, the mechanism of which needs to be further studied.

As stated, the complex index (CI) and/or the loading capacity of target compound have been often considered as important index to determine extent of complex formation [40,41]. Hereby, we introduced total phenolic content of the complex to describe the complexation of TPP within inulin. And higher content of polyphenols stands for better combination of compounds. It was shown that the phenolic contents of different complexes (treated for 0, 10 and 30 min) were significantly different, but implying the same trend with their particle size. The largest particle corresponded to the highest phenolic loading, reaching to 70 ± 6.5 mg/g after 10 min of ultrasonic treatment (Fig. 2A). In our previous research, it was suggested that 25 kHz of ultrasound cannot destroy the structure of polyphenols, as well as the interaction force with inulin. That is to say, the decrease of phenolic content in the complex may come from the decomposition of polysaccharides, who probably possess lower adsorption capacity on polyphenols. Therefore, we finally selected 25 kHz (40 W, 10 min) as the optimal condition to prepare the product of inulin-TPP complex.

3.3. UV–Vis and IR spectrum of inulin-TPP complex

Referring to the phenolic content of the complex, the mixture of inulin and TPP with the same weight ratio was prepared. The complex treated by ultrasound (25 kHz, 40 W) for 30 min was also measured as control. It can be seen from Fig. 3A that inulin-TPP mixture had a typical absorption around 280 nm, due to the flavanol structure (B-ring) of EGCG and ECG [30,42]. However, after successful grafting, the corresponding peak obviously weakened, because fructo-oligomers have no absorption during 240–400 nm [43]. The presence of polyphenol has been previously evidenced by Folin-Ciocalteu method. Thus, it can be speculated that the complexation modified the ultraviolet properties of phenolic compounds. Moreover, there were no significant changes between two inulin-TPP complexes prepared by ultrasonication, whereas both revealing lower adsorption at 280 nm compared to untreated samples. This finding further proved that ultrasound intensifies the interaction between polysaccharide and polyphenol, changing their flavanolic structures and binding forces to some degree.

As exhibited in Fig. 3B, inulin has a broad peak at 3390 cm^{-1} from the O–H stretching of associated glucose and fructose units in the polysaccharide backbone. The band around 2929 cm^{-1} corresponds to C–H stretch and peak at 1626 cm^{-1} can be assigned to the hydroxyl bending mode [44]. The bands at 1032 cm^{-1} and 933 cm^{-1} correspond to C-O-C and C-O stretching, respectively. However, in case of inulin-TPP complex, two typical peaks of –OH moved to larger wavenumbers, at 3396 cm^{-1} and 1641 cm^{-1} respectively. The C–H stretch shifted to a lower wavenumber at 2920 cm^{-1}. The changes can be attributed to the formation of hydrogen bond from different hydroxyls and are a strong proof for the combination of inulin with polyphenols.

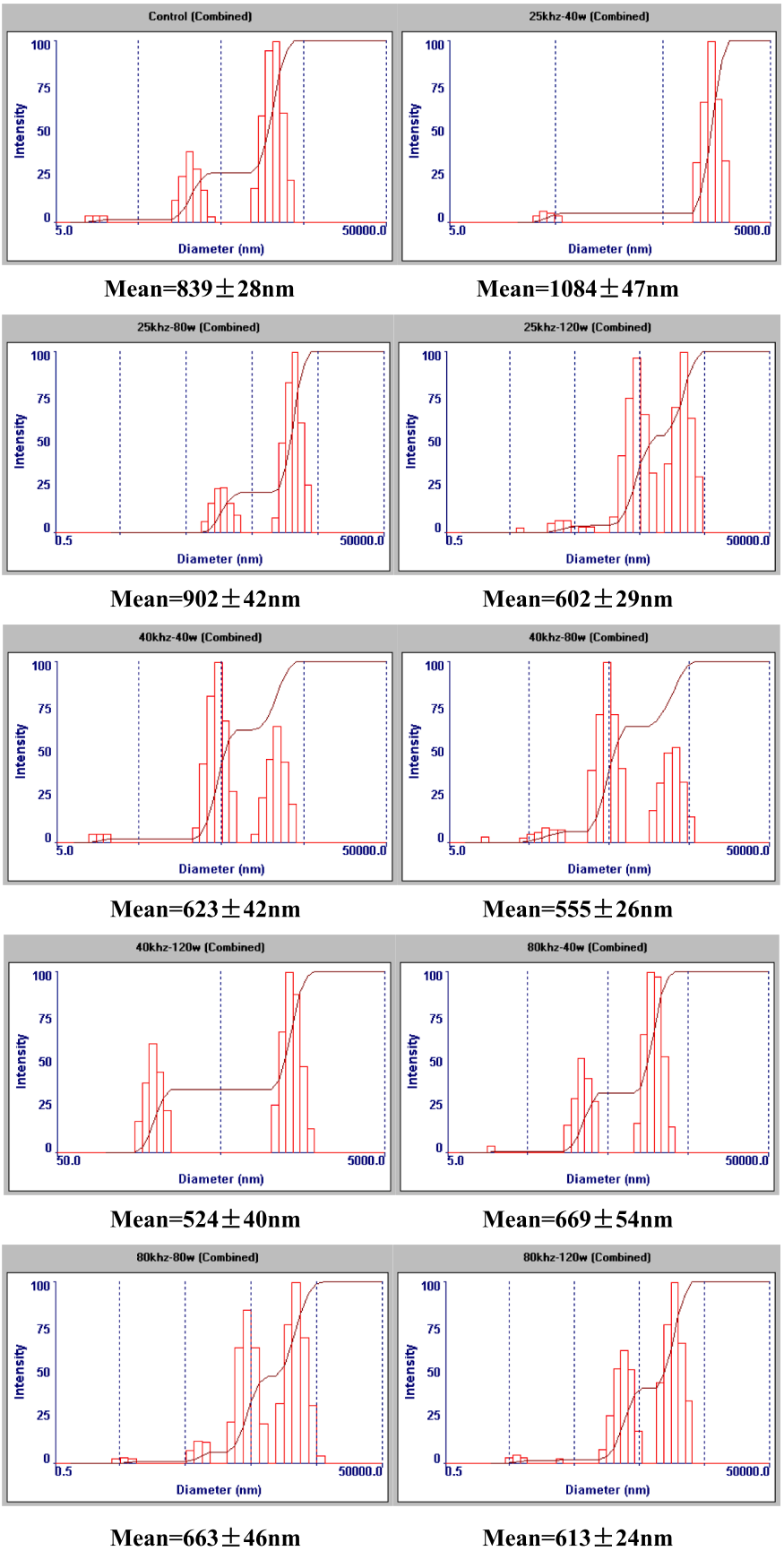

Fig. 1. Particle size distribution and mean diameter (nm) of ultrasound-treated inulin and TPP mixtures under different conditions.

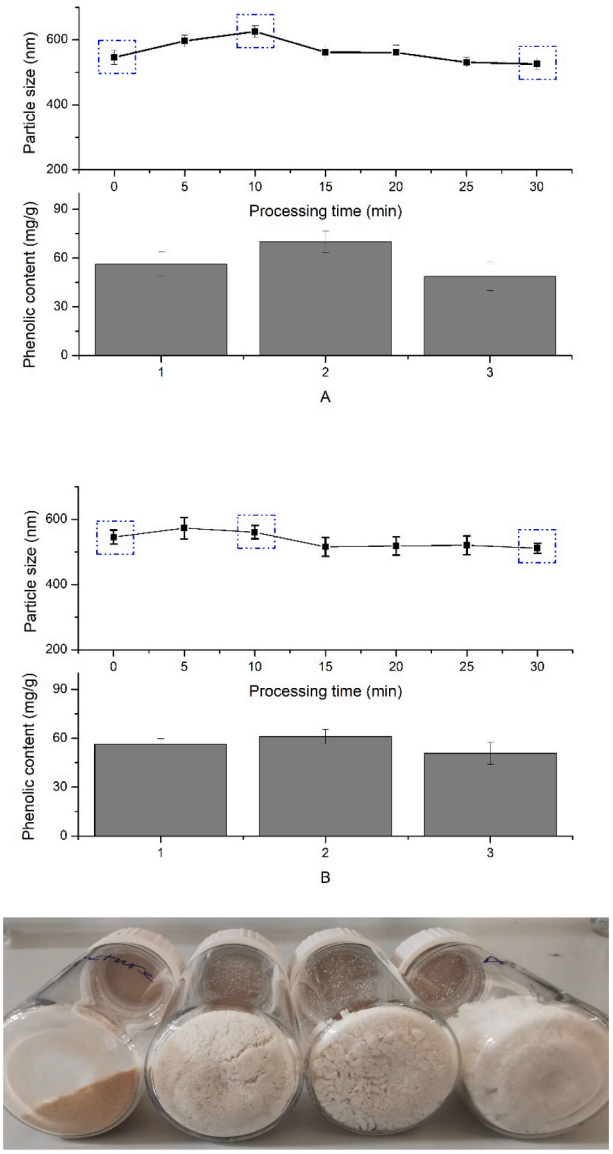

Fig. 2. Average particle size (nm) and phenolic content of inulin-TPP complex treated by 25 kHz, 40 W (A) and 80 W (B) of ultrasound (1, 2, 3 represented different processing times at 0, 10 and 30 min, respectively).

There was no detection of new peaks within 1200–900 cm^{-1} range, indicating that the glycosidic bonds involving C-O-C and C-O stretch between the skeleton of polysaccharides were not altered in the complex [45]. After ultrasonic pretreatment, similar peaks were also found in 40 W-10 min complex at 3412 and 2920 cm^{-1}, both implying the promoting effect of ultrasound on the interaction.

3.4. NMR spectrum of inulin-TPP complex

Three different inulin complexes were identified by NMR analysis, using inulin extract as control. To be mentioned, the inulin applied in this experiment was a maltodextrin-based mixture prior to alcohol precipitation. Thus, its ^{1}H NMR spectrum contained complicated signals that was hard to distinguish (Fig. 4A1). However, the three regions of typical signals were similar to other test compounds. The ^{1}H NMR spectra of inulin-TPP complex without ultrasonic treatment (Fig. 4A2) showed the presence of signal in the anomeric region at 5.24 ppm.

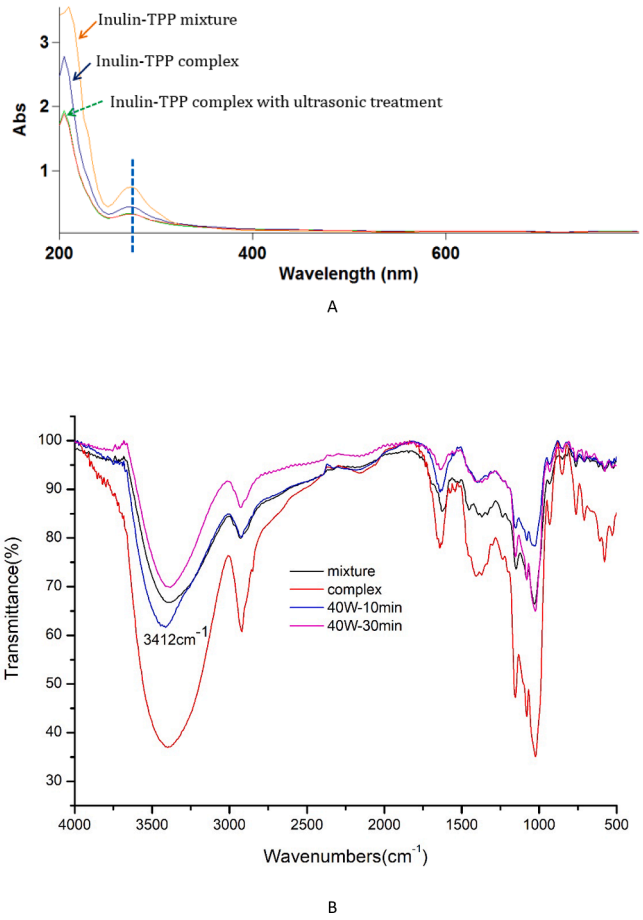

Fig. 3. UV–Vis (A) and FT-IR (B) spectroscopic profiles of different inulin-TPP complexes.

Moreover, intense signals were observed at 4.65 ppm, and in the region between 3.20 and 3.95 ppm. Actually, the previous analysis of inulin extract has revealed its main composition of monosaccharides, including glucose and fructose. Hence, the signals at 5.24 and 4.54 ppm can be assigned as H-1 protons of the α- and β-anomeric forms of free glucose, respectively [46]. The other chemical shifts detected at 3.82, 3.70 and 3.50 ppm represented for fructose units of inulin. The integration of the H-1 signal of the glucose moiety at δ 5.24 ppm and the H-3 and/or H-4 signals of the preponderant fructosyl units between δ 3.20 and 3.95 ppm may provide the mean degree of polymerization (DP) of saccharides involved, possibly from 8 to 10 [47,48]. Comparing the integral ratio between glucose and fructose, it can be found that the peak intense of fructose was decreased after complexation, which implied that the combination of polyphenols with inulin mostly occurs at furan rings depending on hydrogen bond [48]. Additionally, it was revealed that with the introduction of ultrasound, the signal of fructosyl units became even weaker, also verifying the degraded effect of ultrasonic treatment on carbohydrate polymers (Fig. 4A3 & 4). However, there was no observation of significant difference on ^{13}C NMR spectrum of these three different inulin complexes (data not shown), supporting the point that the primary structure of carbohydrate chain was not affected by 25 kHz of ultrasound.

According to DQF-COSY (^{1}H–^{1}H) spectra, the structure of inulin-type fructan can be further confirmed in the complex by the relative signals (Fig. 4B) [49]. The chemical shift of untreated inulin-TPP complex moved to a higher field compared with original extract, which also proved the formation of hydrogen bond between saccharides and phenols (Fig. 4B1 & 2). Furthermore, it was likely that the ultrasound-treated complexes possessed lower DP than untreated ones, which

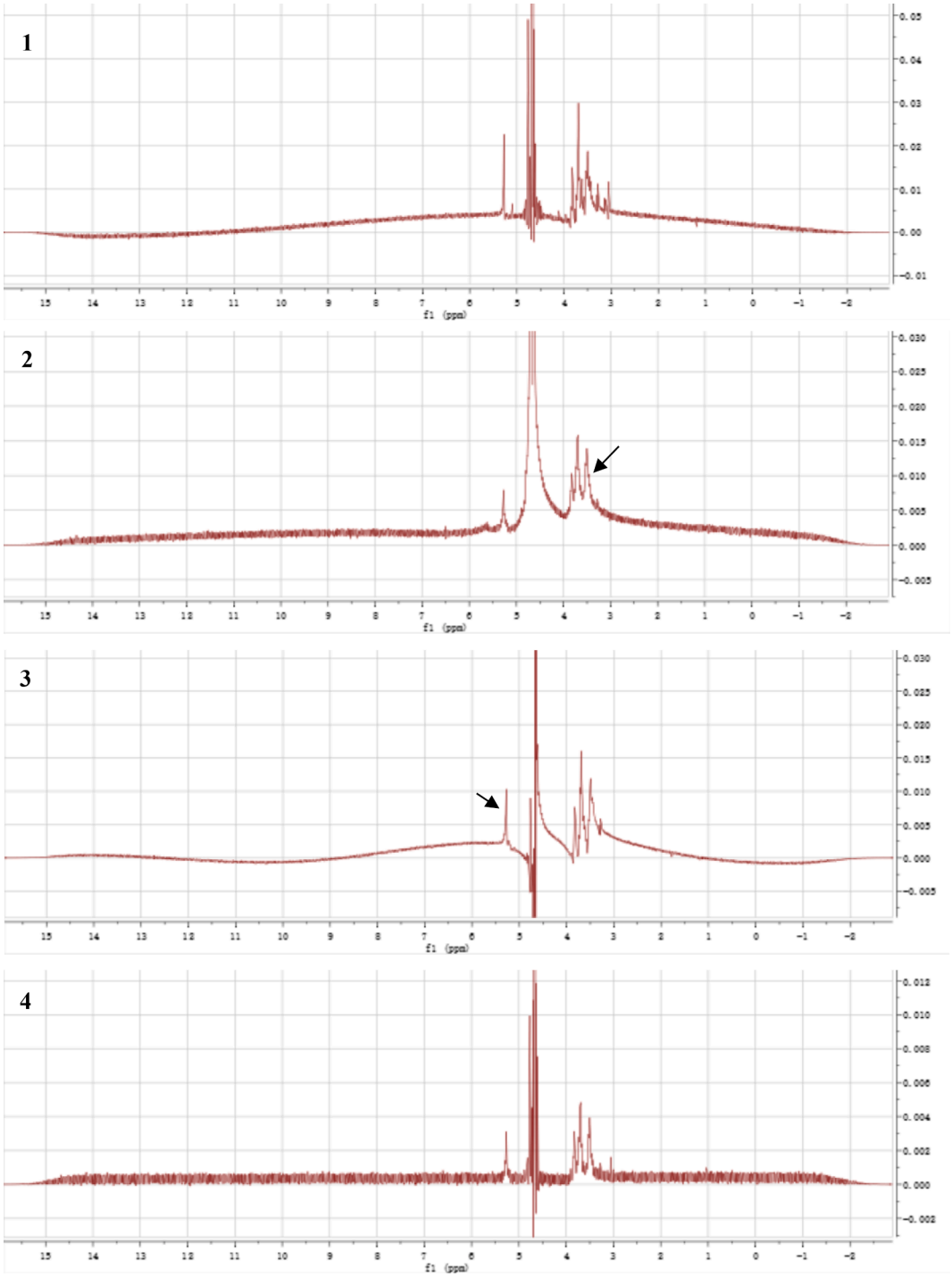

Fig. 4. ^{1}H NMR (A) and DQF-COSY (^{1}H–^{1}H, B) spectra of different inulin-TPP complexes.

needs to be subsequently examined by mass spectrometry [50,51].

3.5. Molecular weight distribution of different complexes

The weight-average molecular weight (Mw) and weight-number molecular weight (Mn) of three different inulin complexes and mixture were analyzed by GPC. The polydispersity of tested samples was all less than 1.8, indicating that the fractions of samples were evenly distributed [52]. Due to the chromatographic profiles, only one fraction with a wide range of mass distribution was obtained from inulin mixture, whereas two main peaks were eluted from other three inulin-TPP complexes. The former one represented the constituent with larger molecular weight (Fig. 5). Hence, it means that after complexed with polyphenols, the relative content of the second eluted peak was decreased significantly, compared to original inulin. Accordingly, the Mw of untreated inulin mixture, inulin-TPP complex, 40 W-10 min and 40 W-30 min complex were 3.395×10^{3}, 2.967×10^{4}, 3.175×10^{4} and 2.985×10^{4} g/mol, respectively. One possible reason for the increasing of the molecular weight might referred to the combination of interacted compounds, such as phenols and their polymers. The other one was

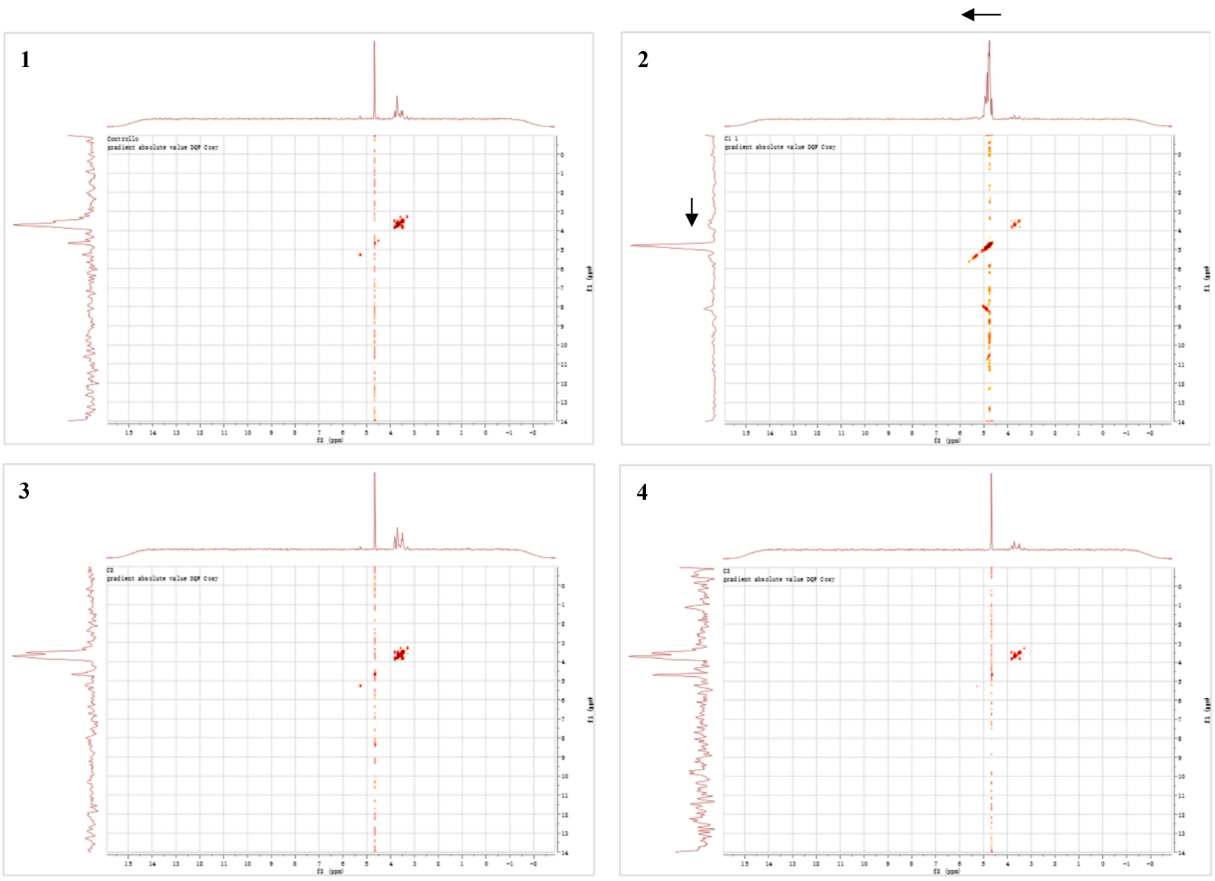

Fig. 4. (*continued*).

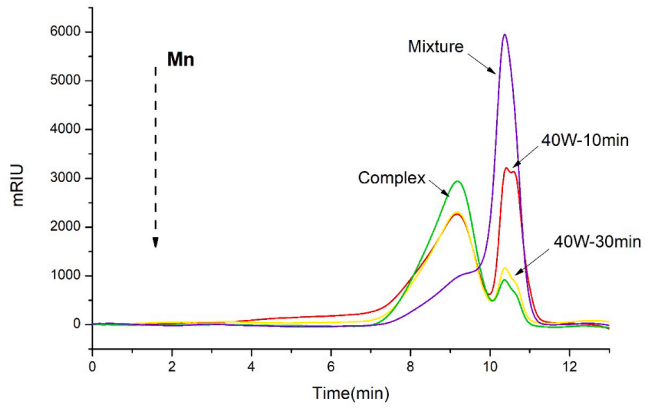

Fig. 5. Molecular weight distribution of different inulin-TPP complexes by GPC analysis.

mostly likely because of the presence of oligosaccharide molecules in inulin extract, which were not removed prior to alcohol precipitation. Spizzirri et al. (2010) found that the molecular weight distribution of inulin was almost unchanged after grafting with catechin, which was probably due to the lower grafting efficiency of the conjugate [53]. But in our study, ultrasound advanced the grafting and interaction of inulin with phenols. In addition, the first eluted peak of ultrasound-treated complex was narrowed, but the second peak was enlarged compared with untreated complex. The phenomenon could be resulted from the degradation effect of ultrasound, which was consistent with the previous conclusion.

3.6. Morphology characteristics of different complexes

Compared with conventional scanning electron microscopy (SEM), field emission SEM (FESEM) produces clearer and less electrostatically distorted images. According to Fig. 6, the morphology of inulin was quite heterogeneous and included a lot of different shapes, which appeared in the form of small balls and roundly shaped bags ranging from some μm up to around 100 μm. There were big elongated particles that seem squeezed bags (with size of about 200 μm × 500 μm) with fibrous composition, and the surface of which was rough (Fig. 6A). However, after combined with polyphenols, obvious difference can be found from the morphology of inulin-TPP complex (Fig. 6B). At lower magnification, the complex appeared in the form of small and elongated shreds, which alternated smooth surfaces with punctured ones. The holes had quite homogeneous size (diameter around 2.5 μm) and seemed regularly arranged. Shi et al. (2020) reported that the irregularly shaped fragments on the surface of starch granules were potential to promote the formation of a complex layer. Furthermore, the interaction between wheat starch and palmitic acid changed the crystal type of starch [54]. The similar phenomenon was also observed in yum starch complex gels, indicating more complex 3D network structure as well as a thinner lamellar membrane [55].

On the other side, the collected images of ultrasound treated-complex presented a slight agglomeration in the form of bent sheets, compared to non-treated sample, which was in accordance with the result of particle size (Fig. 6C). It has been evidenced by Cheng et al. (2018) that complex particle of polysaccharides increased with concentration, also suggesting a gradually broader distribution [56]. To some extent, it could be also resulted from the residual ethanol solvent remained within the material. For 30 min-ultrasound-treated complex, small eroded shreds were detected, which appeared organized to form a

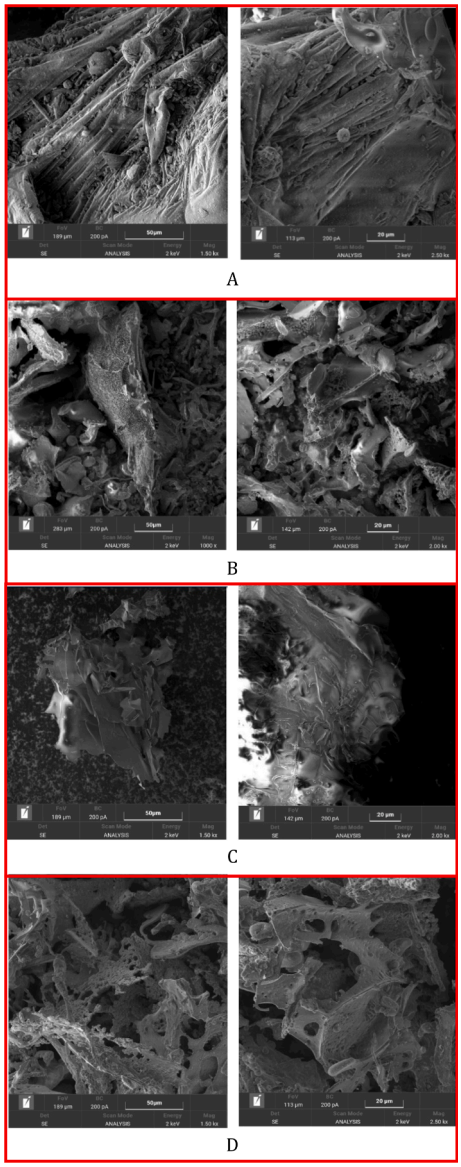

Fig. 6. Morphological characteristics of different inulin-TPP complexes by FESEM analysis at two magnifications.

complicated structure with lace-like morphology (Fig. 6D). In some regions, residual diatom-like appearance has also been observed. It seems that ultrasonic treatment leads to looser and sharp edges, and the prolonged treating time has a beneficial effect on the development of obtained morphology. Zhao et al. (2019) also found that more and more spherulites crystalline formed and gathered as large fragments were destroyed by increasing ultrasound-microwave treatment, which resulted in an opposite effect in the formation of starch complex [35].

3.7. Thermal-stability of different complexes

The TGA curves of inulin-TPP mixture and three complexes were presented in Fig. 7. On account of previous study, the weight loss in thermograph of inulin was composed of three regions. The first region (30–230 °C) corresponded to the weight loss of small amount of moisture in the sample. The second region (230–340 °C) is due to the decomposition of polysaccharides which is followed by a region of complete combustion (340–800 °C). To be mentioned, the second zone lost more than 60% of weight of inulin [57]. However, in the case of complex, four stages of weight loss were present, involving 30–100 °C,

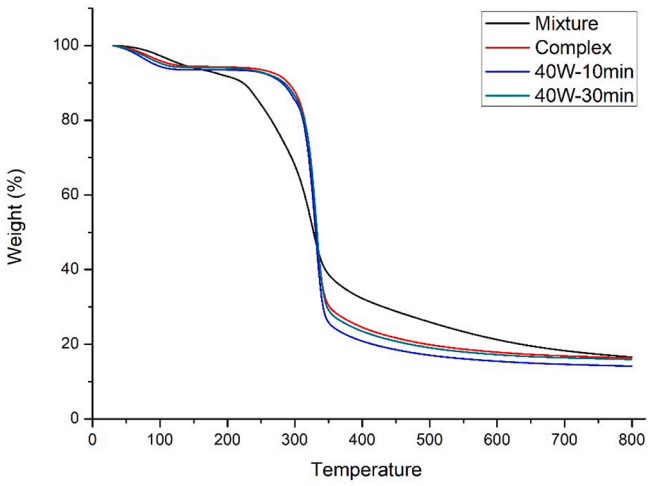

Fig. 7. TGA curves of different inulin-TPP complexes.

100–300 °C, 300–350 °C and 350–800 °C, respectively. Major weight loss (˃70%) in thermograph of complex was attributed to the third region, possibly coming from the depolymerization of inulin and degradation of polyphenols. The first stage was shortened, while the newly generated second stage enhanced the initial temperature of decomposition from 230 to 300 °C. All the results manifest that the inulin-TPP complexes possess better thermal stability than natural inulin [58]. Moreover, only a slight weight loss was observed in the second stage, which also suggested the more stable property of the complex. By the way, at the inflection point between third and fourth stage of thermograph (350 °C), 10 min-treated sample was found to loss approximate 75% of total weight, which was lighter than other complexes, further demonstrating its higher phenolic loading efficiency during complexation.

4. Conclusion

Even though the positive impact of ultrasound on the modification of food component has been evidenced, ultrasonic treatments with different frequencies and output energy present distinct effects on the complexation of polysaccharides and polyphenols. The inulin-TPP complex with highest phenolic loading rate (70.02 ± 6.53 mg/g) was obtained after treated by ultrasound at 25 kHz (40 W, 10 min). However, 40 and 80 kHz of ultrasound decreased the mean diameter of the solutes, simultaneously producing inulin-based solutions with more dispersive size distributions. Based on the identification of inulin-TPP complexes by UV–Vis, FT-IR and NMR analysis, it was shown that the primary structure and polysaccharide skeleton of inulin were not altered in the optimally formed complex. But the degree of polymerization and molecular weight distribution of the complex was influenced by extended ultrasonic treatment. Furthermore, the flavanolic ring of EGCG and ECG in tea polyphenols was possibly modified by complexation, due to the weakened absorption at 280 nm. As a result, the morphological property of the complex was further affected. Diverse FESEM images of complexes and mixture proved the modification of inulin and the promoting effect of ultrasound. Particularly, the thermal stability of ultrasound-treated complex was also improved compared to inulin, possessing higher phenolic content, which supports our previous understanding on the HIU technique. We assume that the complexed-inulin could be an upgraded functional food ingredient with better physicochemical properties in future with the involvement of ultrasound.

CRediT authorship contribution statement

Shuyi Li: Data curation, Writing - original draft. **Dan Lei:** .

Zhenzhou Zhu: Project administration, Funding acquisition. **Jie Cai:** Writing - review & editing. **Maela Manzoli:** Resources. **Laszlo Jicsinszky:** Software. **Giorgio Grillo:** Software. **Giancarlo Cravotto:** Supervision, Funding acquisition.

Declaration of Competing Interest

The authors declare that they have no known competing financial interests or personal relationships that could have appeared to influence the work reported in this paper.

Acknowledgements

The authors thank to the visiting scholar project of China Scholar Council. Financial supports are coming from “Chutian Scholar Plan” and “One Hundred-Talent Program” of Hubei Province, China. The authors also appreciate the support of Outstanding young and middle-aged science and technology innovation team in Hubei Province (T2020012). The study was supported by the University of Turin (ricercar locale 2019).

References

[1] A. Córdova, C. Astudillo-Castro, R. Ruby-Figueroa, P. Valencia, C. Soto, Recent advances and perspectives of ultrasound assisted membrane food processing, Food Res. Int. 133 (2020), 109163.
[2] J.L. Paris, C. Mannaris, M.V. Cabañas, R. Carlisle, M. Manzano, M. Vallet-Regí, C. C. Coussios, Ultrasound-mediated cavitation-enhanced extravasation of mesoporous silica nanoparticles for controlled-release drug delivery, Chem. Eng. J. 340 (2018) 2–8.
[3] Wu, Advances in Ultrasound Technology for Environmental Remediation, Springer, Netherlands, 2013.
[4] X. Fu, T. Belwal, G. Cravotto, Z. Luo, Sono-physical and sono-chemical effects of ultrasound: primary applications in extraction and freezing operations and influence on food components, Ultrason. Sonochem. 104726 (2019).
[5] S. Li, R. Zhang, D. Lei, Y. Huang, S. Cheng, Z. Zhu, Z. Wu, G. Cravotto, Impact of ultrasound, microwaves and high-pressure processing on food components and their interactions, Trends Food Sci. Technol. 109 (2021) 1–15.
[6] K.G. Zinoviadou, C.M. Galanakis, M. BrnI, N. Grimi, N. Boussetta, M.J. Mota, J. A. Saraiva, A. Patras, B. Tiwari, F.J. Barba, Fruit juice sonication: Implications on food safety and physicochemical and nutritional properties, Food Research Int. 77 (2015) 743–752.
[7] F.J. Barba, C.M. Galanakis, M.J. Esteve, A. Frigola, E. Vorobiev, Potential use of pulsed electric technologies and ultrasounds to improve the recovery of high-added value compounds from blackberries, J. Food Eng. 167 (2015) 38–44.
[8] S.A. Sena, K. Bulent, S. Nihan, B. Banu, U.A. Abdullah, A. Cesarettin, Optimizing the extraction parameters of epigallocatechin gallate using conventional hot water and ultrasound assisted methods from green tea, Food Bioprod. Process. 111 (2018) 37–44.
[9] M. Bindes, M. Reis, V.L. Cardoso, D.C. Boffito, Ultrasound-assisted extraction of bioactive compounds from green tea leaves and clarification with natural coagulants (chitosan and Moringa oleífera seeds), Ultrason. Sonochem. (2019).
[10] C.M. Galanakis, Functionality of food components and emerging technologies, Foods 10 (2021) 128.
[11] B. Nazari, M.A. Mohammadifar, S. Shojaee-Aliabadi, E. Feizollahi, L. Mirmoghtadaie, Effect of ultrasound treatments on functional properties and structure of millet protein concentrate, Ultrason. Sonochem. 41 (2018) 382–388.
[12] L. Huang, X. Ding, C. Dai, H. Ma, Changes in the structure and dissociation of soybean protein isolate induced by ultrasound-assisted acid pretreatment, Food Chem. 232 (2017) 727–732.
[13] Y. Xie, J. Wang, Y. Wang, D. Wu, D. Liang, Effects of high-intensity ultrasonic (HIU) treatment on the functional properties and assemblage structure of egg yolk, Ultrason. Sonochem. 60 (2020) 104767.
[14] M. Ulbrich, Y. Bai, E. Flter, The supporting effect of ultrasound on the acid hydrolysis of granular potato starch, Carbohydr. Polym. 230 (2019), 115633.
[15] F. Hou, L. Fan, X. Ma, D. Wang, W. Wang, T. Ding, X. Ye, D. Liu, Degradation of carboxymethylcellulose using ultrasound and β-glucanase: Pathways, kinetics and hydrolysates’ properties, Carbohydr. Polym. 201 (2018) 514–521.
[16] K.M. Albano, N.L.F. Cavallieri, V.R. Nicoletti, Electrostatic Interaction between soy proteins and pectin in O/W emulsions stabilization by ultrasound application, Food Biophys. 15 (2020) 297–312.
[17] K.M. Albano, V.R. Nicoletti, Ultrasound impact on whey protein concentrate-pectin complexes and in the O/W emulsions with low oil soybean content stabilization, Ultrason. Sonochem. (2018). S1350417717304893.
[18] C.M. Galanakis, The food systems in the era of the coronavirus (COVID-19) pandemic crisis, Foods 9 (2020).
[19] C. Cmgab, A. Mr, B. Tmsa, D. Iu, F. Njre, Innovations and technology disruptions in the food sector within the COVID-19 pandemic and post-lockdown era, Trends Food Sci. Technol. (2021).
[20] C.M. Galanakis, T. Aldawoud, M. Rizou, N.J. Rowan, S.A. Ibrahim, Food ingredients and active compounds against the coronavirus disease (COVID-19) pandemic: A comprehensive review, Foods 9 (2020) 1701.
[21] M. Galanakis, Charis, Separation of functional macromolecules and micromolecules: From ultrafiltration to the border of nanofiltration, Trends Food Sci. Technol. 42 (2015) 44–63.
[22] C.M. Galanakis, Phenols recovered from olive mill wastewater as additives in meat products, Trends Food Sci. Technol. 79 (2018) 98–105.
[23] C.M. Galanakis, Implementation of phenols recovered from olive mill wastewater as UV booster in cosmetics, Ind. Crops Prod. 111 (2017) 30–37.
[24] A.B. Md, M.H. Geesi, R. Yassine, I. Mohd, I.A. Md, J.A. Mohamed, A. Noushin, Ultrasound-assisted extraction of some branded tea: Optimization based on polyphenol content, antioxidant potential and thermodynamic study, Saudi J. Biol. Sci 26 (2018). S1319562X18301748.
[25] S. Li, Q. Wu, F. Yin, Z. Zhu, J. He, F. Barba, Development of a combined trifluoroacetic acid hydrolysis and HPLC-ELSD method to identify and quantify inulin recovered from jerusalem artichoke assisted by ultrasound extraction, Appl. Sci. 8 (2018) 710.
[26] D. López-Molina, M.D. Navarro-Martínez, F. Rojas-Melgarejo, A.N.P. Hiner, S. Chazarra, J.N. Rodriguez-Lopez, Molecular properties and prebiotic effect of inulin obtained from artichoke (Cynara scolymus L), Phytochemistry 66 (2005) 1476–1484.
[27] S. Bayarri, I. Chulia, E. Costell, Comparing λ-carrageenan and an inulin blend as fat replacers in carboxymethyl cellulose dairy desserts. Rheological and sensory aspects, Food Hydrocoll. 24 (2010) 578–587.
[28] N. Vural, Z.A. Cavuldak, M.A. Akay, R.E. Anl, Determination of the various extraction solvent effects on polyphenolic profile and antioxidant activities of selected tea samples by chemometric approach, J. Food Meas. Charact. 14 (2020).
[29] Q. Luo, J.R. Zhang, H.B. Li, D.T. Wu, R.Y. Gan, Green extraction of antioxidant polyphenols from green tea (Camellia sinensis), Antioxidants 9 (2020) 785.
[30] S. Li, J. Li, Z. Zhu, S. Cheng, J. He, O. Lamikanra, Soluble dietary fiber and polyphenol complex in lotus root: Preparation, interaction and identification, Food Chem. 314 (2020), 126219.
[31] R.V. Daleffe, M.C. Ferreira, J.T. Freire, Analysis of the effect of particle size distributions on the fluid dynamic behavior and segregation patterns of fluidized, vibrated and vibrofluidized beds, Asia-Pac. J. Chem. Eng. 2 (2010) 3–11.
[32] X. Jia, S. Sun, B. Chen, B. Zheng, Z. Guo, Understanding the crystal structure of lotus seed amylose–long-chain fatty acid complexes prepared by high hydrostatic pressure, Food Res. Int. 111 (2018) 334–341.
[33] S.M.H. Hosseini, Z. Emam-Djomeh, S.H. Razavi, A.A. Moosavi-Movahedi, A. A. Saboury, M.S. Atri, P. Van der Meeren, β-Lactoglobulin–sodium alginate interaction as affected by polysaccharide depolymerization using high intensity ultrasound, Food Hydrocoll. 32 (2013) 235–244.
[34] Q.A. Zhang, X.Z. Fu, J.F. García Martín, Effect of ultrasound on the interaction between (-)-epicatechin gallate and bovine serum albumin in a model wine, Ultrason. Sonochem. 37 (2017) 405.
[35] B. Zhao, S. Sun, H. Lin, L. Chen, S. Qin, W. Wu, B. Zheng, Z. Guo, Physicochemical properties and digestion of the lotus seed starch-green tea polyphenol complex under ultrasound-microwave synergistic interaction, Ultrason. Sonochem. 52 (2019) 50–61.
[36] I.S. Arvanitoyannis, K.V. Kotsanopoulos, A.G. Savva, Use of ultrasounds in the food industry–Methods and effects on quality, safety, and organoleptic characteristics of foods: A review, Critic. Rev. Food Sci. Nutrit. (2015).
[37] Y. Xu, L. Zhang, Y. Yang, X. Song, Z. Yu, Optimization of ultrasound-assisted compound enzymatic extraction and characterization of polysaccharides from blackcurrant, Carbohydr. Polym. (2015).
[38] W. Wang, W. Chen, M. Zou, R. Lv, D. Wang, F. Hou, H. Feng, X. Ma, J. Zhong, T. Ding, Applications of power ultrasound in oriented modification and degradation of pectin: A review, J. Food Eng. 234 (2018) 98–107.
[39] A. Mika, B.N. Greenwood, M. Chichlowski, D. Borchert, K.A. Hulen, B.M. Berg, M. Paton, M. Fleshner, 155. Dietary prebiotics increase Bifidobacterium spp. and Lactobacillus spp. in the gut and promote stress resistance, Brain Behav. Immun. 40 (2014) e45-e45.
[40] K. Kawai, S. Takato, T. Sasaki, K. Kajiwara, Complex formation, thermal properties, and in-vitro digestibility of gelatinized potato starch–fatty acid mixtures, Food Hydrocoll. 27 (2012) 228–234.
[41] R. Shaddel, J. Hesari, S. Azadmard-Damirchi, H. Hamishehkar, B. Fathi-Achachlouei, Q. Huang, Use of gelatin and gum Arabic for encapsulation of black raspberry anthocyanins by complex coacervation, Int. J. Biol. Macromol. 107 (2018) 1800–1810.
[42] S. Sang, M.J. Lee, Z. Hou, C.T. Ho, C.S. Yang, Stability of tea polyphenol (-)-epigallocatechin-3-gallate and formation of dimers and epimers under common experimental conditions, J. Agric. Food Chem. 53 (2005) 9478–9484.
[43] J. Liu, R. Bai, Y. Liu, X. Zhang, J. Kan, C. Jin, Isolation, structural characterization and bioactivities of naturally occurring polysaccharide–polyphenolic conjugates from medicinal plants—A reivew, Int. J. Biol. Macromol. (2017). S0141813017324303.
[44] W.-D. Wang, C. Li, Z. Bin, Q. Huang, L.-J. You, C. Chen, X. Fu, R.H. Liu, Physicochemical properties and bioactivity of whey protein isolate-inulin conjugates obtained by Maillard reaction, Int. J. Biol. Macromol. 150 (2020) 326–335.
[45] A.C. Apolinário, E.M. de Carvalho, B.P.G. de Lima Damasceno, P.C.D. da Silva, A. Converti, A. Pessoa, J.A. da Silva, Extraction, isolation and characterization of inulin from Agave sisalana boles, Ind. Crops Prod. 108 (2017) 355–362.
[46] S. Cérantola, N. Kervarec, R. Pichon, C. Magné, M.A. Bessieres, E. Deslandes, NMR characterisation of inulin-type fructooligosaccharides as the major water-soluble

carbohydrates from Matricaria maritima (L.), Carbohydr. Res. 339 (2004) 2445–2449.
[47] N.T. Petkova, P. Denev, Characterization of inulin from dahlia tubers isolated by microwave and ultrasound-assisted extractions, Int. Food Res. J. 25 (2018) 1876–1884.
[48] Z. Yang, J. Hu, M. Zhao, Isolation and quantitative determination of inulin-type oligosaccharides in roots of Morinda officinalis, Carbohydr. Polym. 83 (2011) 1997–2004.
[49] M. Matulova, S. Husarova, P. Capek, M. Sancelme, A.M. Delort, NMR structural study of fructans produced by Bacillus sp. 3B6, bacterium isolated in cloud water, Carbohydr. Res. 346 (2011) 501–507.
[50] X. Cha, S. Han, J. Yu, S. Zhang, S. Yu, D. Fu, M. Yao, L. Zhang, G. Feng, Inulin with a low degree of polymerization protects human umbilical vein endothelial cells from hypoxia/reoxygenation-induced injury, Carbohydr. Polym. 216 (2019) 97–106.
[51] Y. Meng, Y. Xu, C. Chang, Z. Qiu, J. Hu, Y. Wu, B. Zhang, G. Zheng, Extraction, characterization and anti-inflammatory activities of an inulin-type fructan from Codonopsis pilosula, Int. J. Biol. Macromol. 163 (2020) 1677–1686.
[52] M. Gaborieau, P. Castignolles, Size-exclusion chromatography (SEC) of branched polymers and polysaccharides, Anal. Bioanal. Chem. (2010).
[53] U.G. Spizzirri, O.I. Parisi, F. Iemma, G. Cirillo, F. Puoci, M. Curcio, N. Picci, Antioxidant–polysaccharide conjugates for food application by eco-friendly grafting procedure, Carbohydr. Polym. 79 (2010) 333–340.
[54] S. Shi, Y. Dong, Q. Li, T. Liu, X. Yu, Morphology, structural, thermal and rheological properties of wheat starch–palmitic acid complexes prepared during steam cooking, RSC Adv. 10 (2020) 30087–30093.
[55] R. Zhou, H. Bao, Y.-H. Kang, Synergistic rheological behavior and morphology of yam starch and Auricularia auricula-judae polysaccharide-composite gels under processing conditions, Food Sci. Biotechnol. 26 (2017) 883–891.
[56] H. Cheng, Z. Fang, T. Liu, Y. Gao, L. Liang, A study on β-lactoglobulin-triligand-pectin complex particle: Formation, characterization and protection, Food Hydrocoll. 84 (2018) 93–103.
[57] R. Rahul, U. Jha, G. Sen, S. Mishra, Carboxymethyl inulin: A novel flocculant for wastewater treatment, Int. J. Biol. Macromol. 63 (2014) 1–7.
[58] Y. Jing, J. Huang, X. Yu, Preparation, characterization, and functional evaluation of proanthocyanidin-chitosan conjugate, Carbohydr. Polym. 194 (2018) 139–145.